

On the Instrument Profile of Slit Spectrographs

R. Casini¹ and A. G. de Wijn¹

¹*High Altitude Observatory, National Center for Atmospheric Research,*^a

P.O. Box 3000, Boulder, CO 80307-3000

We derive an analytic expression for the instrument profile of a slit spectrograph, also known as the line spread function. While this problem is not new, our treatment relies on the operatorial approach to the description of diffractive optical systems, which provides a general framework for the analysis of the performance of slit spectrographs under different illumination conditions. Based on our results, we propose an approximation to the spectral resolution of slit spectrographs, taking into account diffraction effects and sampling by the detector, which improves upon the often adopted approximation based on the root-sum-square of the individual contributions from the slit, the grating, and the detector pixel.

PACS numbers: 300.0300,070.0070

arXiv:1409.0137v1 [physics.optics] 30 Aug 2014

^a The National Center for Atmospheric Research is sponsored by the National Science Foundation

I. INTRODUCTION

The quantitative analysis of spectroscopic data from observations demands knowledge of the instrument profile of the spectrographic tools used for data acquisition. The instrument profile determines the spectral resolution of the observations, which ultimately affects the sensitivity of measurements of physically relevant plasma quantities, such as line widths (e.g., radiative, collisional, thermal, plasma turbulence), line shifts (e.g., isotopic, Doppler, gravitational), and spectral modulations in both intensity and polarization (e.g., Zeeman and Stark splitting by applied fields, spectral line polarization in anisotropic media, redistribution of radiation frequency in partially coherent scattering).

In particular, the instrument profile of a slit-based spectrograph, also called the *line spread function* (LSF), depends on the aperture of the entrance slit, the *finesse* of the spectral profile of the dispersive element (e.g., prism, diffraction grating), and the sampling length of the imaged spectrum at the detector (e.g., the pixel size of a CCD camera, or the average size of film grains).

Often, for computational convenience, the simplistic assumption is made that the width of the instrument profile (typically, its *full width at half maximum*, FWHM) can be calculated as the *root-sum-square* (RSS) of the individual contributions from the slit, the chromatic dispersion profile, and the detector's sampling (see, e.g., [1, 2]). This approximation is of course based on the assumption that the profiles associated with each of these contributions can be represented by Gaussian distributions, and that there are no inter-dependences among those contributions. While this assumption may turn out to be valid in some particular configurations of a slit-based spectrograph, it is not representative of the general dispersive and imaging properties of a given instrument. In particular, this approximation cannot properly account for the different diffraction conditions that the experimenter encounters when exploring a very large interval of wavelengths – say, from the extreme blue to the near infrared – while using a fixed aperture of the slit. It also fails to reproduce the different sampling regimes at the detector that necessarily occur in such multi-wavelength usage of the spectrograph, and which may not correspond exactly to the desired sampling condition (e.g., pixel matching, Nyquist sampling).

In this note, we investigate the diffraction properties of a spectrograph in order to arrive at a general expression for the LSF, and ultimately to an analytic approximation to the spectral resolution of the instrument. Obviously, we must rely on the Fourier analysis of the instrument's components. The problem is not new, and in fact we re-derive known results that date at least as far back as Wadsworth's extensive investigation of the effects of the slit aperture on the shape of

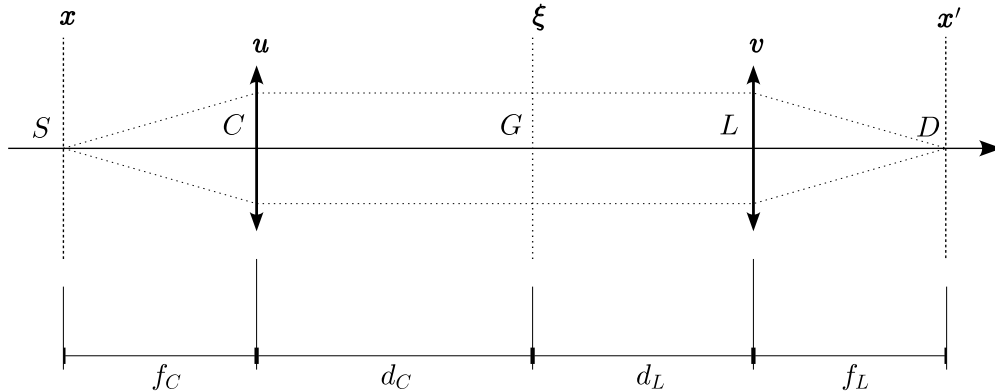


FIG. 1. Layout of the imaging system. See text for details.

spectral lines [3] (see also [4, 5] and references therein). However, for our treatment of the problem, we adopted the tools of the operational calculus of Fourier optics (e.g., [6, 7], and references therein), which lead to a very general and compact description of the *optical transfer operator* (OTO) of a slit spectrograph, opening the ground for further investigations of the performance of such instruments under different illumination conditions, through both analytic and numerical approaches.

In Sect. II we derive the general LSF of a slit spectrograph under the hypothesis of coherent illumination, and obtain a closed analytic form for the case where the grating defines the limiting aperture of the system. We then show how this approach immediately leads to the expression of the LSF in the case of incoherent illumination. Finally, in Sect. III we propose a functional form for the FWHM of the instrument profile after sampling by the detector, for the purpose of estimating the spectral resolution of the instrument.

II. DERIVATION OF THE LINE SPREAD FUNCTION

We consider a slit spectrograph (see Fig. 1), consisting of a slit (S), a collimator lens (C), a grating (G), a camera lens (L), and a detector (D). We assume that the spectrograph can be described operationally as a linear system \mathcal{S} acting on the input field U at the slit, and producing an output field U' at the detector, so that $U' = \mathcal{S}U$. The OTO for such a system, assumed to be perfectly stigmatic (i.e., free of optical aberrations), takes the form (see [6], and the Appendix)

$$\mathcal{S} = \mathcal{R}(f_L) \mathcal{Q}\left(-\frac{1}{f_L}\right) \mathbf{1}_L \mathcal{R}(d_L) \mathbf{1}_G \mathcal{R}(d_C) \mathbf{1}_C \mathcal{Q}\left(-\frac{1}{f_C}\right) \mathcal{R}(f_C) \mathbf{1}_S . \quad (1)$$

Here the operator $\mathcal{Q}(-1/f)$ describes the wavefront modification introduced by a powered optic of focal length f , whereas $\mathcal{R}(d)$ describes the free-space propagation of the wavefront along the

optical path of length d (see the Appendix). Equation (1) does not take into account the presence of beam-limiting apertures along the optical path. The location of those apertures is marked by the presence of the unit operator.

We want to determine the instrument profile (or LSF) for a given wavelength, λ . Using the transformation rules of the operational calculus of Fourier optics (see Appendix), and introducing the dimensional constant $k = 1/(\lambda^2 f_L f_C)$, we find, apart from a constant phase factor,

$$\begin{aligned}
\mathcal{S} &= k \left\{ \mathcal{Q} \left(\frac{1}{f_L} \right) \mathcal{V} \left(\frac{1}{\lambda f_L} \right) \mathcal{F} \mathcal{Q} \left(\frac{1}{f_L} \right) \right\} \mathcal{Q} \left(-\frac{1}{f_L} \right) \mathbf{1}_L \left\{ \mathcal{F}^{-1} \mathcal{Q} \left(-\lambda^2 d_L \right) \mathcal{F} \right\} \mathbf{1}_G \\
&\quad \times \left\{ \mathcal{F}^{-1} \mathcal{Q} \left(-\lambda^2 d_C \right) \mathcal{F} \right\} \mathbf{1}_C \mathcal{Q} \left(-\frac{1}{f_C} \right) \left\{ \mathcal{Q} \left(\frac{1}{f_C} \right) \mathcal{V} \left(\frac{1}{\lambda f_C} \right) \mathcal{F} \mathcal{Q} \left(\frac{1}{f_C} \right) \right\} \mathbf{1}_S \\
&= k \mathcal{Q} \left(\frac{1}{f_L} \right) \mathcal{V} \left(\frac{1}{\lambda f_L} \right) \mathcal{F} \mathbf{1}_L \left\{ \mathcal{F}^{-1} \mathcal{Q} \left(-\lambda^2 d_L \right) \mathcal{F} \right\} \mathbf{1}_G \\
&\quad \times \left\{ \mathcal{F}^{-1} \mathcal{Q} \left(-\lambda^2 d_C \right) \mathcal{F} \right\} \mathbf{1}_C \mathcal{V} \left(\frac{1}{\lambda f_C} \right) \mathcal{F} \mathcal{Q} \left(\frac{1}{f_C} \right) \mathbf{1}_S, \tag{2}
\end{aligned}$$

where \mathcal{F} represents the operation of Fourier transform, and $\mathcal{V}(c)$ is the scaling operator by the quantity c (see Appendix).

In order to develop the OTO expression beyond the general form of Eq. (2), we need to make some assumptions on the transmission functions of the various apertures. First of all, we will assume that the camera lens, L , is sized such as not to introduce any vignetting of the beam after the collimator lens and the grating. In such cases, we can assume that the diameter of the camera lens is virtually infinite, and noting that $\mathcal{F} \mathbf{1}_L \mathcal{F}^{-1} = 1$, we can rewrite,

$$\begin{aligned}
\mathcal{S} &= k \mathcal{Q} \left(\frac{1}{f_L} \right) \mathcal{V} \left(\frac{1}{\lambda f_L} \right) \mathcal{Q} \left(-\lambda^2 d_L \right) \mathcal{F} \mathbf{1}_G \\
&\quad \times \left\{ \mathcal{F}^{-1} \mathcal{Q} \left(-\lambda^2 d_C \right) \mathcal{F} \right\} \mathbf{1}_C \mathcal{V} \left(\frac{1}{\lambda f_C} \right) \mathcal{F} \mathcal{Q} \left(\frac{1}{f_C} \right) \mathbf{1}_S. \tag{3}
\end{aligned}$$

In fact, because the beam between C and L is collimated, we can safely assume that the vignetting of the beam is produced only by the smallest size aperture in the collimator. This can be either the collimator lens, or the grating surface. In the first case, Eq. (3) becomes, using $\mathcal{F} \mathbf{1}_G \mathcal{F}^{-1} = 1$,

$$\begin{aligned}
\mathcal{S}_C &= k \mathcal{Q} \left(\frac{1}{f_L} \right) \mathcal{V} \left(\frac{1}{\lambda f_L} \right) \mathcal{Q} \left(-\lambda^2 [d_L + d_C] \right) \mathcal{F} \mathbf{1}_C \mathcal{V} \left(\frac{1}{\lambda f_C} \right) \mathcal{F} \mathcal{Q} \left(\frac{1}{f_C} \right) \mathbf{1}_S \\
&= k \mathcal{Q} \left(\frac{1}{f_L} \right) \mathcal{Q} \left(-\frac{d_L + d_C}{f_L^2} \right) \mathcal{V} \left(\frac{1}{\lambda f_L} \right) \mathcal{F} \mathbf{1}_C \mathcal{V} \left(\frac{1}{\lambda f_C} \right) \mathcal{F} \mathcal{Q} \left(\frac{1}{f_C} \right) \mathbf{1}_S \\
&= k \mathcal{Q} \left(\frac{1}{f_L^2} [f_L - d_L - d_C] \right) \mathcal{V} \left(\frac{1}{\lambda f_L} \right) \mathcal{F} \mathbf{1}_C \mathcal{V} \left(\frac{1}{\lambda f_C} \right) \mathcal{F} \mathcal{Q} \left(\frac{1}{f_C} \right) \mathbf{1}_S, \tag{4}
\end{aligned}$$

where in the second line we used the commutation property of \mathcal{Q} and \mathcal{V} , and in the third line the group property of \mathcal{Q} . This expression shows that the field reaching the collimator lens is a

scaled Fourier transform (FT) of the input field multiplied by the slit transmission function and an exponential phase factor determined by the focal length f_C . Then the signal that is transferred down to the detector is another scaled FT, followed by another phase factor, which, however, is inessential for the determination of the LSF of the spectrograph.

The alternate approach is to assume that the only limiting aperture is the one imposed by the finite size of the grating. In such case we can ignore the aperture of the collimator lens, but the manipulation of Eq. (3) is somewhat more complicated than in the case leading to Eq. (4). We make use of the following relations,

$$\mathcal{F}^{-1} = \mathcal{V}(-1) \mathcal{F} = \mathcal{F} \mathcal{V}(-1), \quad (5)$$

$$\mathcal{F} \mathcal{V}\left(\frac{1}{\lambda f_C}\right) \mathcal{F} = \mathcal{F}^2 \mathcal{V}(\lambda f_C) \equiv \mathcal{V}(-1) \mathcal{V}(\lambda f_C) = \mathcal{V}(-\lambda f_C), \quad (6)$$

through which Eq. (3) transforms into

$$\begin{aligned} \mathcal{S}_G &= k \mathcal{Q}\left(\frac{1}{f_L}\right) \mathcal{V}\left(\frac{1}{\lambda f_L}\right) \mathcal{Q}(-\lambda^2 d_L) \mathcal{F} \mathbf{1}_G \mathcal{F} \mathcal{V}(-1) \mathcal{Q}(-\lambda^2 d_C) \mathcal{V}(-\lambda f_C) \mathcal{Q}\left(\frac{1}{f_C}\right) \mathbf{1}_S \\ &= k \mathcal{Q}\left(\frac{1}{f_L}\right) \mathcal{Q}\left(-\frac{d_L}{f_L^2}\right) \mathcal{V}\left(\frac{1}{\lambda f_L}\right) \mathcal{F} \mathbf{1}_G \mathcal{F} \mathcal{V}(-1) \mathcal{V}(-\lambda f_C) \mathcal{Q}\left(-\frac{d_C}{f_C^2}\right) \mathcal{Q}\left(\frac{1}{f_C}\right) \mathbf{1}_S \\ &= k \mathcal{Q}\left(\frac{1}{f_L} \left[1 - \frac{d_L}{f_L}\right]\right) \mathcal{V}\left(\frac{1}{\lambda f_L}\right) \mathcal{F} \mathbf{1}_G \mathcal{F} \mathcal{V}(\lambda f_C) \mathcal{Q}\left(\frac{1}{f_C} \left[1 - \frac{d_C}{f_C}\right]\right) \mathbf{1}_S \\ &= k \mathcal{Q}\left(\frac{1}{f_L} \left[1 - \frac{d_L}{f_L}\right]\right) \mathcal{V}\left(\frac{1}{\lambda f_L}\right) \mathcal{F} \mathbf{1}_G \mathcal{V}\left(\frac{1}{\lambda f_C}\right) \mathcal{F} \mathcal{Q}\left(\frac{1}{f_C} \left[1 - \frac{d_C}{f_C}\right]\right) \mathbf{1}_S. \end{aligned} \quad (7)$$

The optical configuration described by this last expression has an advantage for the determination of the spectrograph's instrument profile. We note that, just like in the case of Eq. (4), the transfer of the field amplitude from the slit plane to the vignetting aperture is again a scaled FT of the input field multiplied by the slit transmission function and by an exponential phase factor. However, in this case, the distance of the grating from the collimator lens can be chosen so that $d_C = f_C$, in which case the phase factor is equal to 1. Then the system can be described operationally as a scaled FT of the illuminated slit aperture, which is then multiplied by the grating transfer function, and then further FT-ed and magnified onto the detector. The final phase factor again is inessential for the determination of the spectrograph's LSF. In fact, this phase factor could effectively be reduced to 1 as well, although the necessary condition $d_L = f_L$ may be hard to meet in realistic spectrograph designs, because f_L must be subject to the constraint of the spatial/spectral sampling requirement, and thus it is driven by the pixel size of the detector.

For the following development, we must introduce explicitly the transmission functions of the various apertures. If we use Eq. (4) for the computation of the spectrograph's LSF, and ignore the

final phase factor, we then have

$$\begin{aligned}
\mathcal{S}_C U &= k \mathcal{V} \left(\frac{1}{\lambda f_L} \right) \mathcal{F} t_C \mathcal{V} \left(\frac{1}{\lambda f_C} \right) \mathcal{F} \mathcal{Q} \left(\frac{1}{f_C} \right) t_S U \\
&= k \mathcal{V} \left(\frac{1}{\lambda f_L} \right) \mathcal{F} t_C \mathcal{F} \mathcal{V} (\lambda f_C) \mathcal{Q} \left(\frac{1}{f_C} \right) t_S U \\
&\equiv k \mathcal{V} \left(\frac{1}{\lambda f_L} \right) \mathcal{F} t_C p = k \mathcal{V} \left(\frac{1}{\lambda f_L} \right) (\tilde{t}_C * \tilde{p}) ,
\end{aligned} \tag{8}$$

where in the last line we defined $p \equiv \mathcal{F} \mathcal{V} (\lambda f_C) \mathcal{Q} (1/f_C) t_S U$, and used the convolution theorem (the symbol “ \sim ” indicates the operation of FT, and “ $*$ ” is the convolution product). Using the rules given in the Appendix,

$$\tilde{p} = \mathcal{F}^2 \mathcal{V} (\lambda f_C) \mathcal{Q} (1/f_C) t_S U \equiv \mathcal{V} (-\lambda f_C) \mathcal{Q} (1/f_C) t_S U , \tag{9}$$

so that (cf. Eq. [39])

$$\begin{aligned}
\mathcal{S}_C U &= k \mathcal{V} \left(\frac{1}{\lambda f_L} \right) \tilde{t}_C * \mathcal{V} \left(\frac{1}{\lambda f_L} \right) \tilde{p} \\
&= k \left(\tilde{t}_C \circ \left[\frac{1}{\lambda f_L} \right] \right) * \mathcal{V} \left(-\frac{f_C}{f_L} \right) \mathcal{Q} \left(\frac{1}{f_C} \right) t_S U \\
&= k \left(\tilde{t}_C \circ \left[\frac{1}{\lambda f_L} \right] \right) * \mathcal{Q} \left(\frac{f_C}{f_L^2} \right) \mathcal{V} \left(-\frac{f_C}{f_L} \right) t_S U \\
&= k \left(\tilde{t}_C \circ \left[\frac{1}{\lambda f_L} \right] \right) * \mathcal{Q} \left(\frac{f_C}{f_L^2} \right) \left(t_S \circ \left[-\frac{f_C}{f_L} \right] \right) \left(U \circ \left[-\frac{f_C}{f_L} \right] \right) .
\end{aligned} \tag{10}$$

where we indicated with “ \circ ” the operation of function composition.

Using instead Eq. (7) with $d_C = f_C$, and again ignoring the final phase factor, we find, with a manipulation similar to the previous one,

$$\begin{aligned}
\mathcal{S}_G U &= k \mathcal{V} \left(\frac{1}{\lambda f_L} \right) \mathcal{F} t_G \mathcal{V} \left(\frac{1}{\lambda f_C} \right) \mathcal{F} t_S U = \dots \\
&= k \left(\tilde{t}_G \circ \left[\frac{1}{\lambda f_L} \right] \right) * \left(t_S \circ \left[-\frac{f_C}{f_L} \right] \right) \left(U \circ \left[-\frac{f_C}{f_L} \right] \right) .
\end{aligned} \tag{11}$$

Hence, the field amplitude at the detector, for the two cases where the limiting aperture is provided, respectively, by the collimator or the grating, becomes

$$U_C(\mathbf{x}') = k \int d\boldsymbol{\chi} \tilde{t}_C \left(\frac{1}{\lambda f_L} (\mathbf{x}' - \boldsymbol{\chi}) \right) \exp \left(i \frac{\pi}{\lambda} \frac{f_C}{f_L^2} |\boldsymbol{\chi}|^2 \right) t_S \left(-\frac{f_C}{f_L} \boldsymbol{\chi} \right) U \left(-\frac{f_C}{f_L} \boldsymbol{\chi} \right) , \tag{12}$$

$$U_G(\mathbf{x}') = k \int d\boldsymbol{\chi} \tilde{t}_G \left(\frac{1}{\lambda f_L} (\mathbf{x}' - \boldsymbol{\chi}) \right) t_S \left(-\frac{f_C}{f_L} \boldsymbol{\chi} \right) U \left(-\frac{f_C}{f_L} \boldsymbol{\chi} \right) . \tag{13}$$

For the purpose of this work, we consider the simplest case of a fully coherent, input radiation field of unit amplitude, i.e., $U(\mathbf{x}) = 1$. Then, in the case of Eq. (13), the field amplitude at the detector is given by the convolution of the slit transfer function (a box)—projected onto the

detector, and properly scaled by the spectrograph magnification—with the FT of the grating aperture (a “sinc” function; see [6]). That expression can be formally integrated in terms of the “sine integral” function, $\text{Si}(\theta)$,

$$U_G(x', y') = \frac{1}{\pi^2} \left[\text{Si} \left(\frac{\pi}{2} \frac{w_S/f_C - 2x'/f_L}{\lambda/w_G} \right) + \text{Si} \left(\frac{\pi}{2} \frac{w_S/f_C + 2x'/f_L}{\lambda/w_G} \right) \right] \\ \times \left[\text{Si} \left(\frac{\pi}{2} \frac{h_S/f_C - 2y'/f_L}{\lambda/h_G} \right) + \text{Si} \left(\frac{\pi}{2} \frac{h_S/f_C + 2y'/f_L}{\lambda/h_G} \right) \right], \quad (14)$$

where we indicated with w_S and w_G the full widths of the slit and the grating aperture, respectively, and with h_S and h_G the corresponding full heights. The $\text{Si}(\theta)$ function satisfies the parity condition $\text{Si}(-\theta) = -\text{Si}(\theta)$, and for $\theta > 0$ it can be approximated using the relation

$$\text{Si}(\theta) = \frac{\pi}{2} - f(\theta) \cos \theta - g(\theta) \sin \theta, \quad (15)$$

along with rational approximations of $f(\theta)$ and $g(\theta)$ that are given for $\theta \geq 1$ [8]. For $|\theta| < 1$, we can use the following power expansion (expressed, for computational convenience, through Horner’s algorithm),

$$\text{Si}(\theta) \approx \theta \left(1 - \frac{\theta^2}{6} \left(\frac{1}{3} - \frac{\theta^2}{20} \left(\frac{1}{5} - \frac{\theta^2}{294} \right) \right) \right), \quad (16)$$

which guarantees a precision better than $\sim 3 \times 10^{-7}$. (This can be seen by considering the next order in the power expansion (16), which is bounded by $1/(6 \times 20 \times 42 \times 648)$; see [8].) For an infinitely long slit ($h_S \gg |y| = |y'|f_C/f_L$), taking into account that $\text{Si}(\theta) \rightarrow \pi/2$ in the limit of $\theta \rightarrow \infty$, we find more simply

$$U_G(x', y') \rightarrow U_G(x') = \frac{1}{\pi} \left[\text{Si} \left(\frac{\pi}{2} \frac{w_S/f_C - 2x'/f_L}{\lambda/w_G} \right) + \text{Si} \left(\frac{\pi}{2} \frac{w_S/f_C + 2x'/f_L}{\lambda/w_G} \right) \right]. \quad (17)$$

This last result is in agreement with previous theoretical studies of the problem of coherent illumination of a spectrograph slit and of the determination of the corresponding LSF [4, 5]. The advantage of the operatorial approach adopted here is that the characteristics of the spectrograph are all contained in the OTO of Eqs. (4) and (7), regardless of the form of the input field. This makes for a very compact derivation of the various results, and also improves the traceability of the various hypotheses and approximations involved.

The description of the spectrograph as a combination of linear operators also greatly facilitates the programming of numerical codes for the diffraction analysis of spectrographs. In particular, computational tests using a two-dimensional numerical implementation of the general OTO of Eq. (2) demonstrate our former argument that *the FWHM of the LSF of the spectrograph is principally affected by the smallest of the limiting apertures in the collimator*, regardless of whether this

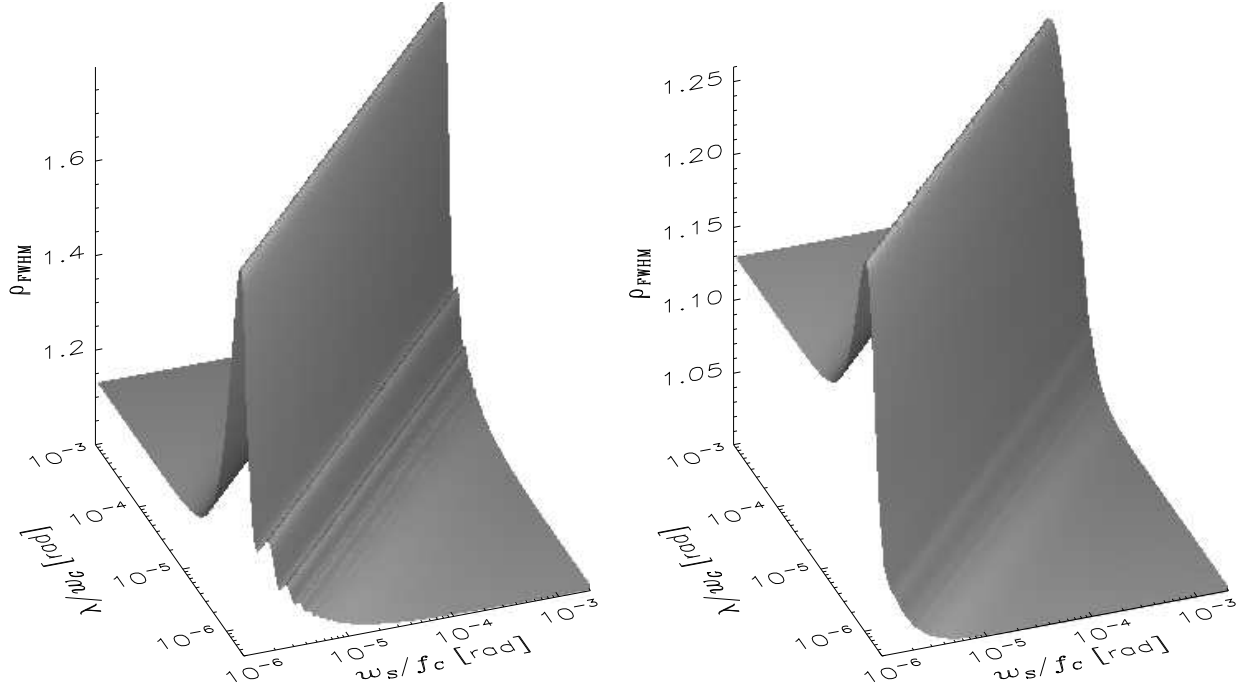


FIG. 2. The ratio ρ_{FWHM} between the RSS estimate of the FWHM of the spectrograph LSF and the exact value as calculated with the model presented in this work, plotted as a function of the two contributions $\gamma_S = w_S/f_C$ and $\gamma_G = \lambda/w_G$: (left) case of coherent illumination; (right) case of incoherent illumination.

aperture corresponds to the collimator lens or the grating (or the camera lens), thus supporting the general applicability of Eq. (17), as soon as we identify w_G with the width of such an aperture. That same code has also been used to validate the model of spectral resolution presented in Sect. III.

The simple analytic expression for the slit image at the detector given by Eq. (17) provides a convenient and accurate method to estimate the *normalized* FWHM of the instrument profile, $\Delta x'/f_L$, for the purpose of computing the resolution of a spectrograph. We note that this FWHM is a function of only two dimensionless parameters, $\gamma_S = w_S/f_C$ and $\gamma_G = \lambda/w_G$, the former representing the angular spread of the slit width as seen by the collimator, while the latter corresponds to the FWHM of the diffraction profile corresponding to the aperture of the grating (or other limiting aperture in the spectrograph).

The left panel of Fig. 2 shows the ratio between the RSS estimate and the exact value of the FWHM of the instrument profile $|U_G(x')|^2$, as a function of the two parameters γ_S and γ_G . The parameter ranges encompass a large set of spectrograph configurations. The range of γ_S spans from, say, a $5\ \mu\text{m}$ slit aperture with a collimator of 5 m focal length, to a 0.5 mm slit aperture with a collimator of only 25 cm focal length. The range of γ_G spans from, say, a wavelength

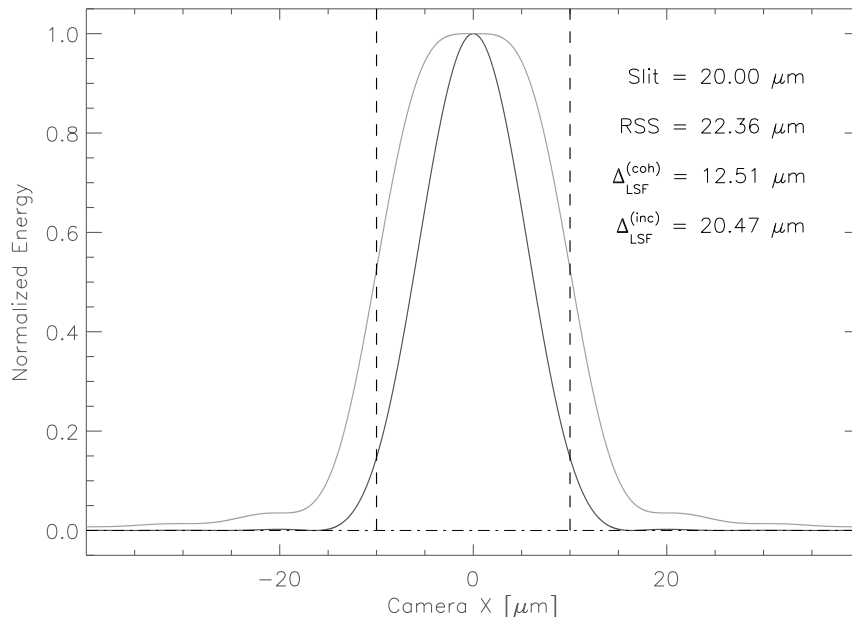


FIG. 3. Cross-section of the energy distribution at the detector (normalized to unit peak), from a fully illuminated slit, for a typical spectrograph configuration ($\lambda = 1 \mu\text{m}$, $w_S = 50 \mu\text{m}$, $f_C = 2.5 \text{ m}$, $w_G = 0.1 \text{ m}$, $f_L = 1 \text{ m}$). The black (gray) curve is for the case of coherent (incoherent) illumination. The figure also gives the projected geometric slit width, and the RSS estimate of the FWHM.

of 200 nm with a grating aperture of 50 cm, to a wavelength of $25 \mu\text{m}$ with a grating aperture of only 2.5 cm. This plot demonstrates the error that can be expected when the FWHM of the instrument profile is approximated by the RSS of the γ_S and γ_G contributions. We also see that this approximation becomes accurate for large slit widths (relative to the focal length of the collimator) and/or small wavelengths (relative to the size of the grating), i.e., when diffraction effects are comparatively unimportant. On the other hand, for small slit apertures and/or large wavelengths the RSS approximation consistently overestimates (by about 13%) the true FWHM. The maximum error that is incurred by using the RSS approximation in intermediate cases is an overestimation of the true FWHM by about 80%, in the case of coherent illumination.

The black curve in Figure 3 shows the LSF at the detector (normalized to unit peak), as calculated through Eq. (17), for a typical spectrograph configuration corresponding to $\gamma_S = 2 \times 10^{-5} \text{ rad}$ and $\gamma_G = 10^{-5} \text{ rad}$ (see caption). The location of this configuration in the domain of Fig. 2 falls in the region where the departure between the true FWHM and its RSS estimate is the largest for coherent illumination. The figure also reports the geometrically projected slit (in this case, corresponding to a spectrograph magnification $f_L/f_C = 0.4$).

In the application of Eq. (17) to realistic grating spectrographs, the two parameters γ_S and γ_G

must in general be multiplied by the *anamorphic magnification*, $r = \cos \alpha / \cos \beta$, where α and β are respectively the incident and diffraction angles of the radiation measured from the grating normal. Alternatively, if $\Delta x'$ is the linear FWHM of the profile of Eq. (17), the actual FWHM of the LSF at the detector plane, $\Delta x'_r$, is determined by the condition $\Delta x' = \Delta x'_r / r$. We note in particular that $r \gamma_G = (\lambda / \cos \beta) / (w_G / \cos \alpha) \equiv \lambda / (L \cos \beta)$, where L is the effective width of the illuminated grating area (rather than its projected width, w_G). As expected, this quantity corresponds to the FWHM of the grating profile function (see, e.g., Eq. [3-6] in [9]).

A. The Case of Incoherent Illumination

Because Eq. (13) has the form of a convolution product of the input field (weighted by the slit aperture) with the translationally invariant kernel

$$h(\mathbf{x}', \mathbf{x}) = \tilde{t}_G \left(\frac{1}{\lambda f_L} (\mathbf{x}' - \mathbf{x}) \right), \quad (18)$$

it follows in particular that $h(\mathbf{x}', \mathbf{x})$ represents the *impulse response* of the linear system describing the spectrograph, under the current assumption that the limiting aperture is provided by the grating. This enables a straightforward description of the behavior of the spectrograph also in the case of fully incoherent illumination, since in such case [6]

$$I_G(\mathbf{x}') = A^{-1} \int d\mathbf{x} |h(\mathbf{x}', \mathbf{x})|^2 t_S(\mathbf{x}) I(\mathbf{x}), \quad (19)$$

where $I(\mathbf{x})$ and $I_G(\mathbf{x}')$ are the field *intensity* at the entrance slit and at the detector, respectively, and A is a normalization constant corresponding to the area of the aperture. Hence, in the case of incoherent illumination, the result analog to Eq. (13) is

$$I_G(\mathbf{x}') = \frac{k}{w_G h_G} \int d\boldsymbol{\chi} \left| \tilde{t}_G \left(\frac{1}{\lambda f_L} (\mathbf{x}' - \boldsymbol{\chi}) \right) \right|^2 t_S \left(-\frac{f_C}{f_L} \boldsymbol{\chi} \right) I \left(-\frac{f_C}{f_L} \boldsymbol{\chi} \right). \quad (20)$$

Remarkably, also this expression can be formally integrated in terms of the sine integral function.

For simplicity of notation, we introduce the following dimensionless quantities,

$$\theta_x^\pm = \frac{\pi}{2} \frac{w_S / f_C \pm 2x' / f_L}{\lambda / w_G}, \quad \theta_y^\pm = \frac{\pi}{2} \frac{h_S / f_C \pm 2y' / f_L}{\lambda / h_G}. \quad (21)$$

We then find explicitly

$$\begin{aligned} I_G(x', y') = & \frac{1}{\pi^2} \left[\text{Si}(2\theta_x^-) + \text{Si}(2\theta_x^+) - \frac{\sin^2 \theta_x^-}{\theta_x^-} - \frac{\sin^2 \theta_x^+}{\theta_x^+} \right] \\ & \times \left[\text{Si}(2\theta_y^-) + \text{Si}(2\theta_y^+) - \frac{\sin^2 \theta_y^-}{\theta_y^-} - \frac{\sin^2 \theta_y^+}{\theta_y^+} \right]. \end{aligned} \quad (22)$$

This expression must be compared with the result of Eq. (14),

$$U_G(x', y') = \frac{1}{\pi^2} \left[\text{Si}(\theta_x^-) + \text{Si}(\theta_x^+) \right] \left[\text{Si}(\theta_y^-) + \text{Si}(\theta_y^+) \right], \quad (23)$$

which is instead valid in the case of coherent illumination. Similarly, in the limit of infinitely long slit, $\theta_y^\pm \rightarrow \infty$, and Eq. (22) reduces to

$$I_G(x', y') \rightarrow I_G(x') = \frac{1}{\pi} \left[\text{Si}(2\theta_x^-) + \text{Si}(2\theta_x^+) - \frac{\sin^2 \theta_x^-}{\theta_x^-} - \frac{\sin^2 \theta_x^+}{\theta_x^+} \right]. \quad (24)$$

This result corresponds to the one originally derived by [3] (see also [4, 5]). Once again, in the application of Eq. (24) to realistic grating spectrographs, the quantities $\gamma_S = w_S/f_C$ and $\gamma_G = \lambda/w_G$ appearing in the definition of θ_x^\pm , Eq. (21), must be multiplied by the proper anamorphic magnification r .

The right panel of Fig. 2 shows the ratio between the RSS estimate and the exact value of the FWHM of the instrument profile $I_G(x')$, as a function of the two parameters γ_S and γ_G . We note that using the RSS estimate of the FWHM in the incoherent case can lead to an underestimation of the spectral resolution of the instrument by as much as 25%. Correspondingly, the gray curve of Fig. 3 shows the LSF at the detector (normalized to unit peak) in the case of incoherent illumination, for the spectrograph configuration listed in the figure's caption.

It is worth noting that *the FWHMs of the spectrograph LSF for the two cases of coherent and incoherent illumination tend to the same value in both regimes $\gamma_S \gg \gamma_G$ and $\gamma_S \ll \gamma_G$* . For intermediate regimes, the FWHM in the coherent case is *always smaller* than the FWHM in the incoherent case, the latter being larger by as much as 40%.

III. SPECTRAL RESOLUTION

The results of Eqs. (17) and (24) do not take into account the sampling of the LSF by the pixels of the detector. Therefore the FWHM of the instrument profile that is derived from those equations, and which we hereafter indicate with Δ_{LSF} , cannot yet be associated with the effective spectral resolution of the instrument. Let us indicate with ζ the ratio of Δ_{LSF} to the pixel size δ_{cam} of the detector expressed in the same units,

$$\zeta = \frac{\Delta_{\text{LSF}}}{\delta_{\text{cam}}}. \quad (25)$$

We want to be able to model the minimum resolvable spectral interval $\Delta\lambda$ as a function of ζ , so that we can estimate the spectral resolution of the instrument as

$$R(\lambda; \zeta) = \frac{\lambda}{\Delta\lambda(\zeta)}. \quad (26)$$

In order to do this, it is convenient to express Δ_{LSF} and δ_{cam} in wavelength units. If $\delta\beta$ is some angular interval in the diffracted beam, the corresponding wavelength interval for a given spectrograph configuration (α, β) is

$$\delta\lambda = \frac{d\lambda}{d\beta} \delta\beta = \frac{\lambda \cos \beta}{\sin \alpha + \sin \beta} \delta\beta, \quad (27)$$

where in the last equivalence we used the expression of the angular dispersion $d\beta/d\lambda$, which is derived from the grating equation. In the following, we assume that both quantities Δ_{LSF} and δ_{cam} have been converted to wavelength units through the transformation (27). Of course, if those quantities were originally given in linear units, they must first be transformed to angular units through division by f_L .

Knowledge of the detailed physical behavior of the function $\Delta\lambda(\zeta)$ in Eq. (26) is often not necessary, if we are only interested in approximately estimating the spectral resolution of the instrument (say, within 10%). This is the case, for example, in many spectrographic applications to the remote sensing of astrophysical plasmas. On the other hand, the function $\Delta\lambda(\zeta)$ must always satisfy the two following limit conditions: 1) for very small ζ , the LSF of the instrument is completely undersampled, and the spectral resolution is thus determined by the detector's pixel size, so that

$$\lim_{\zeta \rightarrow 0} \Delta\lambda(\zeta) \approx 2\delta_{\text{cam}}, \quad (28)$$

where the (approximate) factor 2 enters because of the Nyquist criterion; 2) for very large ζ , the LSF is fully resolved by the detector, and therefore the spectrograph resolution is simply determined by Δ_{LSF} , that is,

$$\lim_{\zeta \rightarrow \infty} \Delta\lambda(\zeta) = \Delta_{\text{LSF}}. \quad (29)$$

We also note that the condition (29) must be approximately satisfied already for relatively small values of ζ , practically as soon as the LSF is critically sampled by the detector, i.e., $\zeta \gtrsim 2$, or $\Delta_{\text{LSF}} \gtrsim 2\delta_{\text{cam}}$. On the other hand, for $\zeta \approx 1$, we have the so-called ‘‘pixel matching’’ condition for a spectrograph, in which $\Delta_{\text{LSF}} \approx \delta_{\text{cam}}$. Under this condition, the minimum resolved spectral interval is evidently $\Delta\lambda \approx 2\Delta_{\text{LSF}} \approx 2\delta_{\text{cam}}$.

We can then conclude that the function $\Delta\lambda(\zeta)$ must remain approximately at the value $2\delta_{\text{cam}}$ for $0 \leq \zeta \lesssim 2$, to then rapidly turn into a linear function of ζ for $\zeta \gtrsim 2$, so that $\Delta\lambda(\zeta) \sim \Delta_{\text{LSF}}$ in that regime. We thus propose the following functional form for $\Delta\lambda(\zeta)$,

$$\Delta\lambda(\zeta) = \delta_{\text{cam}} \sqrt{\zeta^2 + 4 \exp(-\alpha\zeta^q)}, \quad (30)$$

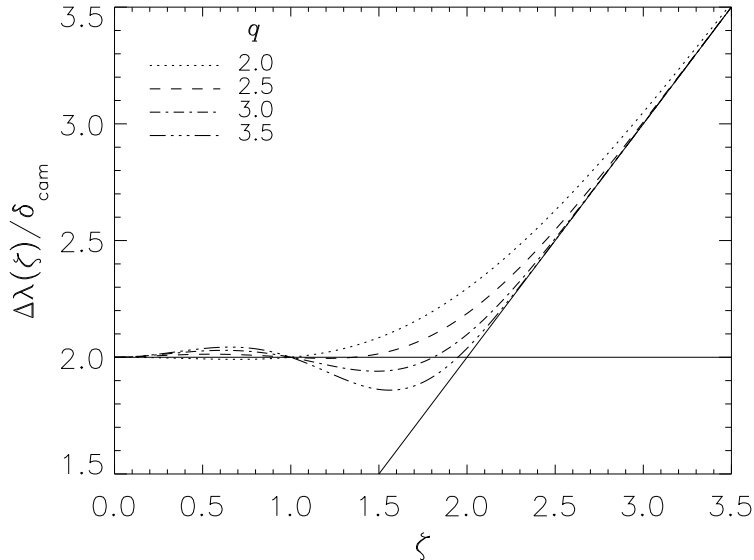


FIG. 4. Plots of Eq. (30) with $\alpha = \ln(4/3)$, for various values of the exponent q . See text for details.

where α and q are two positive quantities. We see that Eq. (30) automatically satisfies the limits (28) and (29). The value of α can be determined by imposing the additional condition that, for pixel matching ($\zeta = 1$), it also must be $\Delta\lambda(1) \approx 2\delta_{\text{cam}}$. If, for simplicity, we assume this condition to be exact, we find

$$\alpha = \ln(4/3) . \quad (31)$$

The parameter q remains undetermined, and can be chosen so to provide a good representation of the qualitative behavior of $\Delta\lambda(\zeta)$ as discussed above. Figure 4 shows the graphs of Eq. (30), with the condition (31), for several values of q . We find that $2.5 \lesssim q \lesssim 3.0$ provides a good choice for approximating the expected behavior of $\Delta\lambda(\zeta)$ as a function of the sampling ratio.

To summarize, we propose the use of the expressions (26) and (30), along with the definition (25), for an improved estimate of the spectral resolution of a slit-based spectrograph, under various regimes of slit diffraction and detector sampling. The FWHM of the instrument profile, Δ_{LSF} , must be computed numerically through Eq. (17) in the case of coherent illumination, and through Eq. (24) in the case of incoherent illumination, after due modification to account for the anamorphic magnification corresponding to the specific configuration of the spectrograph (see discussion at the end of Section II). We suggest a value between 2.5 and 3.0 for the q exponent of ζ in Eq. (30), since this provides a good qualitative agreement with the proposed model of spectral resolution, as it is apparent from the plots of Figure 4.

Figure 5 shows two-dimensional numerical diffraction calculations of the instrument profile of

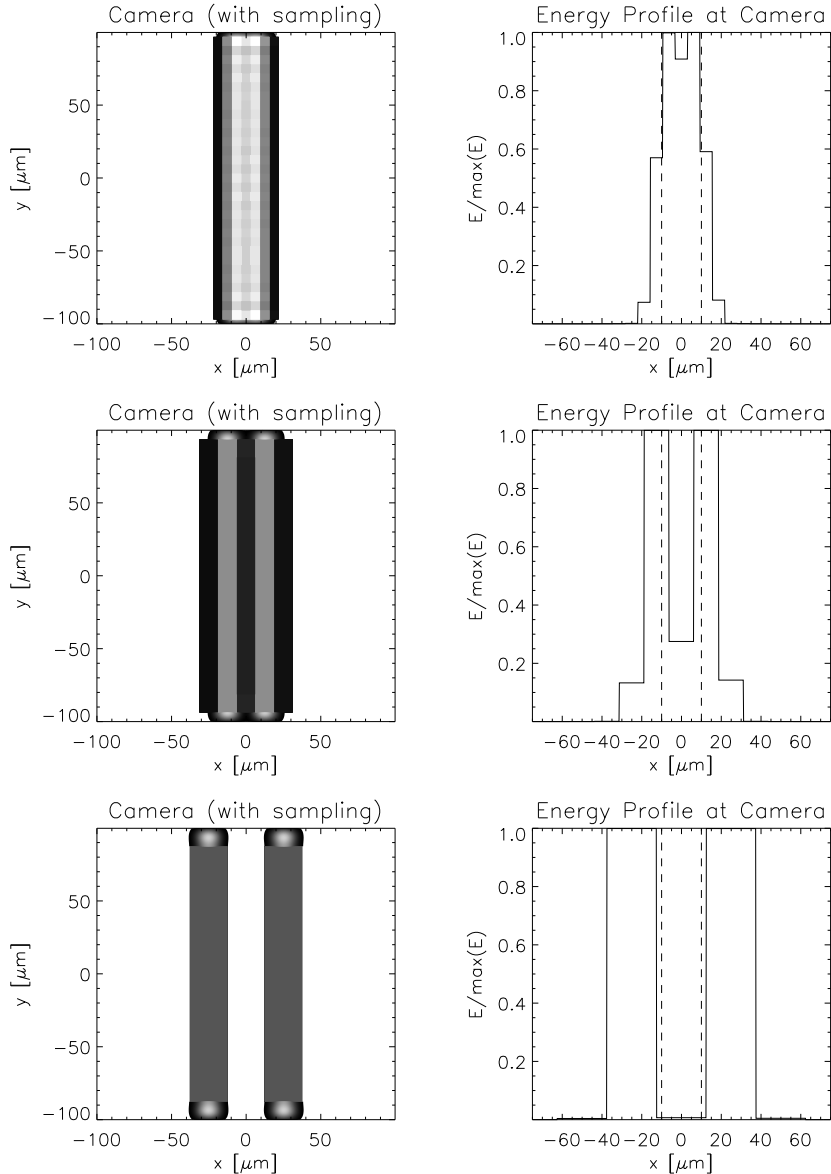


FIG. 5. Numerical tests of the resolution formula Eq. (30), using the same spectrograph configuration of Fig. 3, for three different pixel sizes: $6.25 \mu\text{m}$ (top), $12.5 \mu\text{m}$ (center), and $25 \mu\text{m}$ (bottom), corresponding to $\zeta = 2.0, 1.0, 0.5$, respectively. See text for details. The vertical dashed lines in the panels on the right define the geometric projection of the slit (cf. Fig. 3).

a spectrograph sampled by a detector with which we tested the validity of Eq. (30). For the test, we adopted the same spectrograph configuration, slit width, and wavelength as in the example of Fig. 3, for the case of coherent illumination. We considered three different sampling sizes of the detector's pixel, namely, $\delta_{\text{cam}} = 6.25, 12.5, \text{ and } 25 \mu\text{m}$, corresponding to the cases of $\zeta = 2.0, 1.0, \text{ and } 0.5$, respectively. Finally, we used our numerical code implementing the general OTO

of Eq. (2) to compute the two-dimensional LSF and replicate it at the positions on the detector of two neighboring wavelengths exactly separated by the spectral resolution interval $\Delta\lambda(\zeta)$, as calculated through Eq. (30). In practical cases, the resulting pattern would correspond to two infinitely sharp emission lines that are barely resolvable by the spectrograph. The panels on the left are contour plots of the diffracted energy at the two neighboring wavelengths. Those plots show the appearance of the two infinitely sharp emission lines after being diffracted through the spectrograph and sampled by the detector. We displayed the *unsampled* diffracted field at the very top and bottom pixels of the contour plots, so to help visualize how the detector array aligned with the LSF for each of the test cases. The panels on the right show the cross-cut energy profile (normalized to unit peak amplitude) of the contour plot on the left, for $y = 0$. These calculations show that the two neighboring wavelengths are either fully or just barely resolved, depending on whether the position of the sampling array is more or less optimally aligned with the LSF profile. This is indeed what we must expect from a definition of *minimum* spectral resolution based on the Nyquist criterion.

We want to conclude this section by comparing our results for the resolution of a grating spectrograph with other commonly used expressions that are found in the literature. We refer particularly to the comprehensive treatment of spectrographs presented in [10]. Using the assumptions of that work, the spectral resolution becomes in our notation (cf. Eq. [12.2.3] of [10])

$$R = \frac{\sin \alpha + \sin \beta}{\cos \beta} \frac{w_G}{r w_S} \frac{F}{D}, \quad (32)$$

where D and F are, respectively, the diameter and focal length of the telescope feeding the spectrograph. The “seeing-limited” (s.l.) case corresponds to the regime $\gamma_S \gg \gamma_G$. Hence, diffraction effects from the slit can be ignored, and it is possible to apply the geometric condition $w_G/f_C = D/F$ that corresponds to the conservation of the *etendue* [10]. Equation (32) then becomes

$$R_{\text{s.l.}} = \frac{\sin \alpha + \sin \beta}{\cos \beta} \frac{f_C}{r w_S} = \frac{\sin \alpha + \sin \beta}{\cos \beta} \frac{1}{r \gamma_S}. \quad (33)$$

On the other hand, in the “diffraction-limited” (d.l.) case, $w_S = (\lambda/D)F$, and Eq. (32) becomes

$$R_{\text{d.l.}} = \frac{\sin \alpha + \sin \beta}{\cos \beta} \frac{w_G}{r \lambda} = \frac{\sin \alpha + \sin \beta}{\cos \beta} \frac{1}{r \gamma_G}. \quad (34)$$

If we ignore the sampling of the LSF by the detector, from Eqs. (26) and (27) we find instead that the expression for the spectral resolution has the general form

$$R = \frac{\sin \alpha + \sin \beta}{\cos \beta} \frac{1}{\Delta_{\text{LSF}}}, \quad (35)$$

for all regimes of γ_S and γ_G . Thus our expression coincides with one or the other of Eqs. (33) and (34) only if $\Delta_{\text{LSF}} = r\gamma_S$ or $\Delta_{\text{LSF}} = r\gamma_G$. Our previous analysis has shown that indeed $\Delta_{\text{LSF}} \rightarrow r\sqrt{\gamma_S^2 + \gamma_G^2} \rightarrow r\gamma_S$ when $\gamma_S \gg \gamma_G$, whereas the general expression for Δ_{LSF} never tends to $r\gamma_G$ (see Fig. 2) when $\gamma_S \ll \gamma_G$. To demonstrate this, we can simply consider the case of coherent illumination in the regime $\gamma_S \ll \gamma_G$, since we already noted that both $|U_G(x')|^2$ and $I_G(x')$ give rise to the same Δ_{LSF} in that regime. If we then let $\gamma_S = \epsilon\gamma_G$ in Eq. (17), we find, in the limit $\epsilon \ll 1$,

$$|U_G(x')|^2 \sim \epsilon^2 \text{sinc}^2\left(\frac{x'/f_L}{r\gamma_G}\right), \quad (36)$$

so that $\Delta x'/f_L \approx 0.8859 r\gamma_G$. Therefore, while the use of Eq. (33) is appropriate in the slit-dominated regime of spectrographic observations, the use of Eq. (34) near the diffraction limit leads to an underestimation (by about 13%) of the true spectral resolution (see Fig. 2).

ACKNOWLEDGMENTS

The authors are thankful to P. Nelson and P. Oakley (HAO) for helpful discussions during the investigation of this problem, and to P. Judge (also HAO) for a careful reading of the manuscript and valuable suggestions.

IV. APPENDIX: THE OPERATIONAL CALCULUS OF FOURIER OPTICS

In this Appendix we summarize the main properties of the Fourier operational calculus for the analysis of optical systems [6, 7]. As different authors use slightly different definitions, we decided to adopt the original presentation of [7]. The four basic operations other than the identity are:

1. *Multiplication by a quadratic-phase exponential,*

$$\mathcal{Q}(c)\{f(\mathbf{u})\} = \exp\left(i\frac{\pi}{\lambda}c|\mathbf{u}|^2\right)f(\mathbf{u}), \quad (37)$$

which satisfies the group properties $\mathcal{Q}(a)\mathcal{Q}(b) = \mathcal{Q}(a+b)$ and $\mathcal{Q}(0) = \mathbf{1}$, for any parameters a and b , and operand $f(\mathbf{u})$.

2. *Scaling by a constant,*

$$\mathcal{V}(c)\{f(\mathbf{u})\} = f(c\mathbf{u}), \quad (38)$$

which satisfies the group properties $\mathcal{V}(a)\mathcal{V}(b) = \mathcal{V}(ab)$ and $\mathcal{V}(1) = \mathbf{1}$. We note that, if $h(\mathbf{u}) = f(\mathbf{u}) \otimes g(\mathbf{u})$ (with “ \otimes ” an arbitrary multiplicative operation), then Eq. (38) applied to $h(\mathbf{u})$ implies the distributive property

$$\mathcal{V}(c)\{f(\mathbf{u}) \otimes g(\mathbf{u})\} = \mathcal{V}(c)\{f(\mathbf{u})\} \otimes \mathcal{V}(c)\{g(\mathbf{u})\} . \quad (39)$$

3. *Direct and inverse Fourier Transform (FT),*

$$\mathcal{F}^{\pm 1}\{f(\mathbf{u})\} = \int_{-\infty}^{+\infty} d\mathbf{u} \exp(\mp i 2\pi \mathbf{u}' \cdot \mathbf{u}) f(\mathbf{u}) , \quad (40)$$

with $\mathcal{F}\mathcal{F}^{-1} = \mathcal{F}^{-1}\mathcal{F} = \mathbf{1}$. Obviously, the conjugate variables \mathbf{u} and \mathbf{u}' must satisfy the dimensional relation $[u'] = [u]^{-1}$.

4. *Free-space propagation* of a field $U(\mathbf{x})$ through a distance d ,

$$\mathcal{R}(d)\{U(\mathbf{x})\} = \frac{\exp(i 2\pi d/\lambda)}{i\lambda d} \int_{-\infty}^{+\infty} d\mathbf{x} \exp\left(i \frac{\pi}{\lambda d} |\mathbf{x}' - \mathbf{x}|^2\right) U(\mathbf{x}) , \quad (41)$$

which satisfies the group properties $\mathcal{R}(a)\mathcal{R}(b) = \mathcal{R}(a+b)$ and $\mathcal{R}(0) = \mathbf{1}$. These properties are not self-evident, but they easily follow as a corollary of the equivalence

$$\mathcal{R}(d) = \frac{\exp(i 2\pi d/\lambda)}{i} \mathcal{F}^{-1} \mathcal{Q}(-\lambda^2 d) \mathcal{F} , \quad (42)$$

which is derived from applying the convolution theorem to the expression of Eq. (41). Another useful expression of the free-space propagation operator is the following,

$$\mathcal{R}(d) = \frac{\exp(i 2\pi d/\lambda)}{i\lambda d} \mathcal{Q}\left(\frac{1}{d}\right) \mathcal{V}\left(\frac{1}{\lambda d}\right) \mathcal{F} \mathcal{Q}\left(\frac{1}{d}\right) . \quad (43)$$

The operators listed above satisfy several commutation relations that are useful for the manipulation of chains of operators representing optical systems. Some of these relations, which have been used in these notes, are the following:

$$\mathcal{V}(t) \mathcal{F} = \mathcal{F} \mathcal{V}(1/t) , \quad (44)$$

$$\mathcal{V}(t) \mathcal{Q}(c) = \mathcal{Q}(t^2 c) \mathcal{V}(t) , \quad (45)$$

$$\mathcal{F}^2 = \mathcal{V}(-1) . \quad (46)$$

[1] J. M. Lerner, and A. Thevenon, *The Optics of Spectroscopy: A Tutorial*, Jobin Yvon/Horiba Optical Systems, Metuchen, NJ (1998)

- [2] D. F. Elmore, R. Casini, G. L. Card, M. Davis, A. Lecinski, R. Lull, P. G. Nelson, and S. Tomczyk, "A New Spectro-Polarimeter for Solar Prominence and Filament Magnetic Field Measurements," *SPIE* **7014**, 39-48 (2008)
- [3] F. L. O. Wadsworth, "On the Resolving Power of Telescopes and Spectroscopes for Lines of Finite Width," *Phil. Mag.* **43**, 317-343 (1897)
- [4] P. H. van Cittert, "Zum Einfluß der Spaltbreite auf die Intensitätsverteilung in Spektrallinien," *Z. Phys.* **65**, 547-563 (1930)
- [5] K. D. Mielenz, "Spectroscopy Slit Images in Partially Coherent Light," *J. Opt. Soc. Am.* **57**, 66-71 (1967)
- [6] J. W. Goodman, *Introduction to Fourier Optics* (2nd ed.), McGraw Hill, New York (1996)
- [7] M. Nazarathy, and J. Shamir, "Fourier Optics Described by Operator Algebra," *J. Opt. Soc. Am.* **70**, 150-159 (1980)
- [8] M. Abramowitz, and I. A. Stegun, *Handbook of Mathematical Functions*, National Bureau of Standards, Washington (1964)
- [9] D. F. Gray, *The Observation and Analysis of Stellar Atmospheres*, Wiley, New York (1976)
- [10] D. J. Schroeder, *Astronomical Optics* (2nd ed.), Academic, San Diego (2000)